PB82-236399

Regional Analysis of Factors Affecting Visual Air Quality

(U.S.) Environmental Monitoring Systems Lab.
Las Vegas, NV

2 Feb 81

U.S. Department of Commerce
National Technical Information Service
NTIS

TECHNICAL REPORT DATA
(Please read Instructions on the reverse before completing)

1. REPORT NO.	2.	3. RECI PB82-236399
EPA-600-J-80-149	JOURNAL ARTICLE	

4. TITLE AND SUBTITLE	5. REPORT DATE
REGIONAL ANALYSIS OF FACTORS AFFECTING VISUAL AIR QUALITY	11-3-80
	6. PERFORMING ORGANIZATION CODE: EMSL-LV
7. AUTHOR(S): Ann Pitchford, Advanced Monitoring Systems Division, EMSL	8. PERFORMING ORGANIZATION REPORT NO.: EMSL-LV-214
9. PERFORMING ORGANIZATION NAME AND ADDRESS: Advanced Monitoring Systems Division, Environmental Monitoring Systems Laboratory, P.O. Box 15027, Las Vegas, NV 89114	10. PROGRAM ELEMENT NO.
	11. CONTRACT/GRANT NO.
12. SPONSORING AGENCY NAME AND ADDRESS: Environmental Protection Agency	13. TYPE OF REPORT AND PERIOD COVERED: Journal Article
	14. SPONSORING AGENCY CODE: EPA

15. SUPPLEMENTARY NOTES
Journal Article submitted to Atmospheric Environment, Nov. 1980 Vol. 15, No. 10/11.

16. ABSTRACT

Abstract—The U.S. Environmental Protection Agency, National Park Service, Visibility Research Center, and University of California at Davis are currently operating a monitoring program in national parks and monuments throughout much of the western United States. Project VIEW, the Visibility Investigative Experiment in the West, includes measurement of visibility parameters using manual telephotometers, and measurement of particle concentrations averaged over 72 h. Variation of these parameters occurs in both space and time. To better understand these variations, several techniques including principal component analysis and data comparisons among sites are applied to Fall, 1979 data for much of the network. Then the Grand Canyon is chosen for additional analysis. Best and worst case visibility days are determined and compared with particle concentrations. Finally, hypothetical causes for visibility reduction are further verified by computing wind trajectories back in time for these special case days.

Highlights of this preliminary investigation include evidence that fine sulfur and fine particles are responsible for visibility variation at the VIEW sites; that fine particle copper may be suitable as a tracer for copper smelter impact and that at the Grand Canyon, the majority of trajectories for days of visibility greater than 310 km come from the north and west, over Utah and Nevada.

17. KEY WORDS AND DOCUMENT ANALYSIS

a. DESCRIPTORS	b. IDENTIFIERS/OPEN ENDED TERMS	c. COSATI Field/Group

18. DISTRIBUTION STATEMENT	19. SECURITY CLASS *(This Report)*	21. NO. OF PAGES: 26
	20. SECURITY CLASS *(This page)*	22. PRICE

EPA Form 2220-1 (Rev. 4-77) PREVIOUS EDITION IS OBSOLETE

REPRODUCED BY
NATIONAL TECHNICAL INFORMATION SERVICE
U.S. DEPARTMENT OF COMMERCE
SPRINGFIELD, VA 22161

EPA-600/J-80-149
JOURNAL ARTICLE

Atmospheric Environment Vol. 15, No. 10/11, pp. 2043–2054, 1981
Printed in Great Britain.

REGIONAL ANALYSIS OF FACTORS AFFECTING VISUAL AIR QUALITY*

ANN PITCHFORD, MARC PITCHFORD† and WILLIAM MALM
Environmental Monitoring Systems Laboratory, U.S. Environmental Protection Agency, Las Vegas, Nevada, U.S.A.

ROBERT FLOCCHINI and THOMAS CAHILL
University of California, Davis, California, U.S.A.

and

ERIC WALTHER
Visibility Research Center, John Muir Institute, Las Vegas, Nevada, U.S.A.

(*First received* 16 *September* 1980 *and in final form* 2 *February* 1981)

Abstract—The U.S. Environmental Protection Agency, National Park Service, Visibility Research Center, and University of California at Davis are currently operating a monitoring program in national parks and monuments throughout much of the western United States. Project VIEW, the Visibility Investigative Experiment in the West, includes measurement of visibility parameters using manual telephotometers, and measurement of particle concentrations averaged over 72 h. Variation of these parameters occurs in both space and time. To better understand these variations, several techniques including principal component analysis and data comparisons among sites are applied to Fall, 1979 data for much of the network. Then the Grand Canyon is chosen for additional analysis. Best and worst case visibility days are determined and compared with particle concentrations. Finally, hypothetical causes for visibility reduction are further verified by computing wind trajectories back in time for these special case days.

Highlights of this preliminary investigation include evidence that fine sulfur and fine particles are responsible for visibility variation at the VIEW sites; that fine particle copper may be suitable as a tracer for copper smelter impact and that at the Grand Canyon, the majority of trajectories for days of visibility greater than 310 km come from the north and west, over Utah and Nevada.

INTRODUCTION

In recent years an awareness has developed of the potential conflict in the western United States between accelerated resource development and increased population, and maintenance of the high degree of visual air quality traditionally associated with the West. This has resulted in increasing interest in determining the role of various air pollution sources in visibility degradation. As more has been learned about the causes of visibility degradation, questions about regional scale visibility phenomena have developed. To answer them, it is necessary to establish the spatial and temporal characteristics of regional phenomena and to evaluate the relative impact of both nearby and distant sources on visibility. In an effort to answer these questions the U.S. EPAs Environmental Monitoring Systems Laboratory-Las Vegas (EMSL-LV) in cooperation with the National Park Service, established project VIEW; Visibility Investigative Experiment in the West. This regional scale visibility monitoring and particle sampling network is located in national parks and monuments throughout the Southwest.

The following presentation is a preliminary analysis of some of the visibility and fine particulate data gathered during the initial phases of VIEW. The investigation starts by applying statistical techniques including principal component analysis to the Fall, 1979 visibility and particle data set. Next, temporal variations of visual range at eight of the monitoring sites are compared. Then, the Grand Canyon is chosen for more detailed analysis, and best and worst visibility days are identified for comparison with particle concentrations. Possible causes for visibility reduction are further verified by computing wind trajectories for the several days preceding these best and worst days.

The telephotometer network is operated by the Visibility Research Center, John Muir Institute, affiliated with the University of Nevada, Las Vegas. A description of the network locations, operating procedures, and data handling techniques is given by Malm *et al.* (1980) and Malm (1980). Briefly, instantaneous measurements of contrast between targets and the sky at a wavelength of 550 nm (green) are made three times daily, 9 a.m., noon and 3 p.m. local time, using a manual MRI Vista Ranger™ telephotometer. These data are available from the summer of 1978 to the fall of 1979, in the form of standard visual ranges calculated for each tree-covered target sight path at each monitoring site. Standard visual range is visual

* Paper presented at the Symposium on Plumes and Visibility: Measurements and Model Components. Grand Canyon, Arizona, U.S.A. 10–14 November 1980.

† On assignment from National Oceanic and Atmospheric Administration.

range corrected for a standard "Rayleigh" scattering coefficient of 0.01 km^{-1} (U.S. EPA 1980). Measurements made using targets that are snow covered have been removed from the data set. Thus, data from winter and early spring are not available except for the southernmost network sites, and for uniformity, were not used in this analysis. However, data were not eliminated or sorted according to sky condition (cloudless, partially cloudy, or overcast). Visibilities measured under cloudless conditions are generally higher than those measured under cloudy conditions (Malm *et al.* 1980), but this difference is not critical to the types of analysis used here. The sites and targets used in the analysis for this paper are shown in Fig. 1. Detailed information for the sites is given in Table A1.

The University of California at Davis (Flocchini *et al.*, 1980) installed and operated particle samplers beginning in Fall, 1979 at many of these same sites mentioned above and shown in Fig. 1. The samplers collect two, 72 h duration samples each week. Particles are collected on two filters by particle size (15 to 2.5 μm and less than 2.5 μm diameter, referred to as coarse and fine particles respectively). The samples are weighed and then analyzed by Particle Induced X-ray Emission (PIXE) for elemental constituents larger in atomic weight than sodium. Measured elemental and total gravimetric concentrations are used to calculate two other parameters. For each sample, the sum of the mass of measured elements plus the mass associated with assumed oxide levels for many of the elements defines the total estimated mass (TOTX). (A table of elements and assumed oxide levels used is given in Table A2.) The difference between the gravimetric mass (GRAV) and the total estimated mass yields an estimate of the light element mass (LTE).

To summarize, data from telephotometers are available from the summer of 1978 to the fall of 1979, except for winter, and early spring. In addition, particulate data (72 h averages) are available at many of the visibility monitoring stations from the Fall, 1979 through to Spring, 1980.

STATISTICAL ANALYSIS

When working with large data sets, it is sometimes difficult to extract trends or variations which are common to parameters within the data set. Principal component analysis is one technique that tends to sort out these variations. Determination of principal components (Frane and Hill, 1974; 1976) is a statistical approach to assess whether observed correlations between parameters in a large parameter set can be explained by a few hypothetical variables or factors. The analysis essentially classifies those parameters which tend to vary together as part of a group or factor. The parameters grouped in a factor often suggest an underlying physical interpretation. However, some factors may represent systematic or random errors of measurement. This technique has been used before on constituents of airborne particles (Hopke *et al.*, 1976 and Gaarenstroom *et al.*, 1977) and on particulate sulfates, meteorological, and air quality data (Henry and Hidy, 1979).

The first step in principal component analysis is the generation of a cross correlation matrix of all the

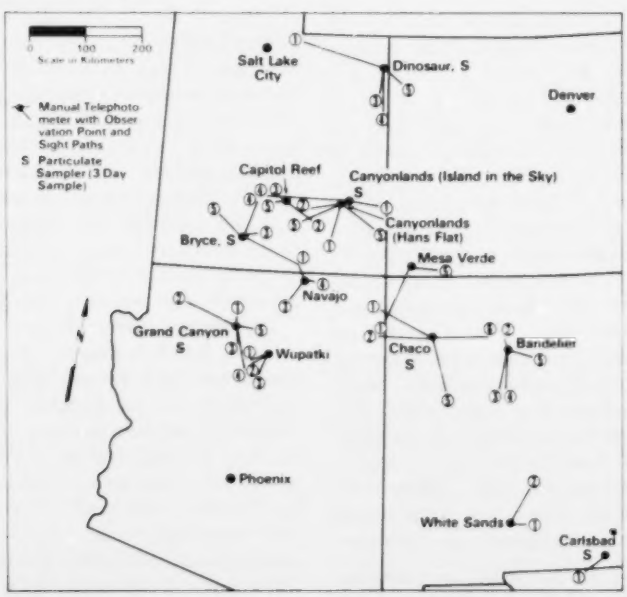

Fig. 1. "VIEW" Monitoring Network Site Map. (A list of sites, target names and distances to targets is given in Table A1.)

variables to be analyzed. The correlation matrices were constructed for each site from a data set which combined particle data with visibility and meteorological data. The telephotometer data (expressed as an extinction coefficient measured for each sight path) and meteorological data were both averaged over the 72 h time period corresponding to the particle samples. A minimum of one valid visibility value per day was required to compute the 72 h average. The particles were characterized in each size range by mass concentrations of the various elements identified, and the parameters TOTX, LTE and GRAV, which were defined earlier. Meteorological data consisted of wind speed and direction values estimated for each station using a daily 7 a.m. Eastern Standard Time National Weather Service 500 mb map. For purposes of the principal component analysis, the wind velocity vector was converted to u and v components referred to as REGIONU, and REGIONV, respectively; wind speed, REGIONWS, was also included as a variable in the analysis. The Fall season was the only time both visibility and particle data were available. This analysis was not possible for the Dinosaur site due to lack of concurrent visibility and particle data. At Canyonlands, the more complete Hans Flat telephotometer data set was substituted for the Island in the Sky data set.

Examination of the results of these analyses shows that at each site, the visibility parameters, i.e., sight path extinction coefficient for the target named, are all grouped in one factor, with various particle parameters. For the purposes of this paper, these joint visibility-particle factors are the most interesting. They are given in Table 1, along with the number of cases at each station and the percent of total variance of the data set explained by that factor. The factors shown contain only parameters with factor loadings of at least 0.5.

First, note that for each sight path, factor loadings (parameters are in decreasing order of factor loading within the factor), vary to some degree. This variation could be due to the contributions of a number of

Table 1. Principal component analysis summary table for five visibility/particulate sites listing only factors containing visibility parameters (Fall, 1979)

Canyonlands Hans Flat n† = 9 variance explained = 34% parameters‡	Bryce Canyon n = 8 variance explained = 47% parameters	Grand Canyon n = 19 variance explained = 36% parameters	Chaco Canyon n = 10 variance explained = 15% parameters	Carlsbad Caverns n = 14 variance explained = 13% parameters
S2	K1	TOTXI	Washington Pass	TOTX2
S1	Fel	Sil	Mt. Taylor	S2
Mt. Holmes	Parker Mt.	Mt. Trumbull	Nacimiento Mts.	−Ca2
TOTX2	Cottonwood	Cal	S1	GRAV2
Mt. Ellen	Sil	Kendrick	Beautiful Mt.	Hunter Pk.
Flank	Cal	LTE2	S2	
Abajos	TOTXI	Fel		
Cul	Til	K1		
Ti2	Ca2	GRAV2*		
−LTE1*	Navajo Mt.	Red Butte		
Cu2	K2	All		
Zn2	GRAV1	GRAV1*		
GRAV2*	Fe2	S2		
−REGIONV	LTE1*	Til*		
	−Cl1			
	TOTX2			
	Table Cliffs Plateau			
	Si2*			
	S2			
	−C12*			
	−Cu2*			
	Nil*			

* Parameter is in more than one factor.

† Number of cases used in principal component analysis.

‡ Parameter abbreviation followed by stage number for particle parameters (Stage 1—15 to 2.5 microns, Stage 2—less than 2.5 microns). Parameters include: elements, gravimetric mass (GRAV), total mass of measured elements with oxides (TOTX) and mass of light elements (LTE) where LTE = GRAV − TOTX. A minus (−) sign indicates a negative factor loading. Target names represent extinction coefficient determined by telephotometer measurements of target specified. Regional winds (500 millibar level) are displayed as REGIONWS for wind speed, REGIONU for vector wind component in the east/west direction (east is positive) and REGIONV for vector wind component in the north/south direction (north is positive). Parameters shown all have factor loadings greater than 0.500.

causes such as spatial inhomogeniety of the air mass surrounding the observation point, variations in inherent contrast that were not accounted for, the observation angle of the target sight path from the horizontal plane, cloud cover, etc. However, an attempt was made to use targets that minimize these effects.

One of the more striking results is that sulfur, for all sites, always falls into the same group as the visibility parameter. In fact, at Chaco Canyon, the only particle components associated with the visibility parameters are coarse and fine sulfur. This suggests but does not prove that sulfur compounds are in part responsible for the variance of the visibility data set. The only thing that is certain is that visibility and sulfur tend to vary together.

A second important variable to be associated with visibility change is fine particulate mass, represented by GRAV2 or TOTX2. Total fine particulates tend to vary with visibility at all sites except Chaco Canyon.

A surprising result at some sites is the inclusion of coarse soils (Fe, Ca, Si, Ti and Al are soil indicators (Pitchford *et al.*, 1980) in the visibility factor. It has been generally accepted that visibility is quite sensitive to particle concentrations in the 0.1 to 1.0 μm diameter range and relatively insensitive to particles outside that range. Yet, the data suggest that the coarse soil particles are related to visibility degradation. Again, this does not prove the coarse soils are necessarily responsible for visibility degradation; but merely indicates that visibility and coarse soil vary together. It is possible that the underlying cause which makes the sulfur and fine particle concentrations vary is the same cause which makes the coarse soil concentrations vary. Alternately, the soil may be directly responsible for the variations in visibility. This may be due to either relatively stable fine particle concentrations during periods of highly variable coarse particle concentration, or higher than theoretically predicted scattering efficiencies for irregular soil particles as suggested elsewhere (Jaggard *et al.* 1980). These hypotheses require further examination, for example, by applying multivariate regression analysis such as that used by Trijonis and Yuan (1978), or Barone *et al.* (1978).

It is also useful to examine in more detail the correlation matrix that was used as input data for the principal component analysis. Table 2 presents correlation coefficients for parameters of interest including coarse and fine soil (Fe was used as a soil indicator), coarse and fine gravimetric mass, and fine sulfur, potassium, copper, and lead, for all the site/target combinations used in the principal component analysis. Although the table shows some similarities among the sites, several of the sites have unique characteristics.

Fine sulfur is the only element that shows a significant correlation with visibility for most, i.e., 11 out

Table 2. Correlation coefficients for telephotometer-measured extinction coefficient vs particle sample components

	Coarse soil	Fine soil	Coarse gravimetric	Fine gravimetric	Fine sulfur	Fine potassium	Fine Light elements	Fine copper	Fine lead
Canyonlandlands									
Hans Flat (n = 9)									
Mt. Holmes	0.403	−0.184	0.151	0.764*	0.950†	−0.219	0.474	0.711*	−0.150
Mt. Ellen Flank	0.483	−0.191	0.239	0.810†	0.937†	−0.248	0.547	0.749*	−0.252
Abajos	0.680*	0.190	0.463	0.852†	0.863†	−0.272	0.617	0.581	−0.414
Bryce (n = 8)									
Navajo Mt.	0.887†	0.753*	0.791*	0.595	0.634	0.849†	0.469	−0.409	−0.009
Table Cliffs Plateau	0.669	0.491	0.543	0.556	0.556	0.611	0.501	−0.331	0.156
Patker Mt.	0.930†	0.753*	0.837†	0.423	0.708*	0.773*	0.245	−0.406	0.249
Cottonwood Peak	0.901†	0.674	0.867†	0.454	0.650	0.814*	0.289	−0.446	0.088
Grand Canyon (n = 19)									
Mt. Trumbull	0.753†	0.422	0.584†	0.685†	0.675†	−0.142	0.652†	−0.012	0.230
Red Butte	0.603†	0.121	0.406	0.579†	0.713†	0.713†	−0.498	−0.049	0.265
Kendrick	0.722†	0.280	0.543*	0.676†	0.774†	−0.219	0.580†	0.021	0.293
Chaco Canyon (n = 10)									
Beautiful Mt.	0.565	0.370	0.538	0.010	0.754*	0.504	−0.142	−0.165	−0.149
Washington Pass	0.301	0.038	0.171	0.030	0.805†	0.323	−0.059	0.076	−0.102
Mt. Taylor	0.114	0.067	0.014	−0.093	0.552	0.306	−0.199	0.277	−0.086
Nacimieno Mt.	0.548	0.427	0.398	0.273	0.763*	0.483	0.119	−0.265	−0.394
Carlsbad (n = 14)									
Hunter Peak	−0.209	−0.151	−0.214	0.472	0.658*	0.272	0.227	0.369	0.305

* Indicates a correlation coeeficient signifciant at the 0.05 level.
† Indicates a correlation coefficient significant at the 0.01 level.
n represents the number of samples.

of 15, site/target combinations. Chaco Canyon and Carlsbad have no other significant correlation. As might be expected from the principal component analysis, coarse soils have significant correlations with visibility at the Bryce and Grand Canyon sites. At some of the locations, the correlation coefficients of coarse soil to fine sulfur (not shown) are significant. This may indicate a possible link between these parameters which might account for the high coarse soil visibility correlation at these sites.

Two of the three remaining locations, Canyonlands and Grand Canyon, indicate significant correlations between visibility and fine gravimetric mass. Canyonlands is the only site where fine copper has a significant correlation with visibility, while Grand Canyon is unique in that fine light elements and coarse soil have significant correlations. Bryce alone has significant correlation coefficients for fine potassium which has been associated with vegetative burning (Lyons *et al.*, 1979).

The correlation table shows no real surprises, but it does serve to highlight distinctive characteristics such as the copper at Canyonlands, the potassium at Bryce, and the fine light elements and coarse soil at Grand Canyon. These particulate characteristics may yield information on the scale of influence of various sources on visibility, and be useful as tracers in determining causes of visibility degradation. However, additional research will be necessary to determine source characteristics.

Many of the relationships shown in the principal component analysis and correlation coefficient tables have not been explained in this brief review. Only obvious parameters such as fine sulfur and coarse soil, have been discussed. Additional analysis awaits a data set containing an entire year of visibility and particulate data.

ANALYSIS OF EXTREME CASES

The statistical analyses treated the data sets in their entirety. This tends to obscure or ignore some of the available information. A useful approach to this type of data is to contrast and compare the characteristics associated with the best and worst day visibility cases. If a characteristic is consistently and markedly different between the two extreme visibility groups, it may be related to the visibility. This technique is applied to one monitoring location, Grand Canyon. In order to suggest the degree to which the analysis for Grand Canyon can be generalized to the rest of the study area time plots of visual range were examined.

Figures 2 and 3 are time plots of visual ranges measured at 8 different sites for the time period starting in late September and continuing on to late October 1979. The visual ranges plotted for Canyonlands, Bryce Canyon, Grand Canyon, and Bandelier represent values measured for the sight path to the target named. These targets were chosen for their regional representativeness. Daily station averages are plotted for the other monitoring stations. These values are computed by finding the geometric mean visual range for all measurement times and targets for a given site and day. Examination of visual range data for these vistas reveals many similar features. At times, within the same general region, the data trends tend to behave in unison while at other times, they tend to behave independently.

Features readily apparent are the frequency and positions of peaks and valleys in the time plots. Especially striking is the highest peak for this time period found simultaneously at all stations on 21st, 22nd and 23rd October. Based on the 1½ years of data available, a network-wide event such as this is rare. Another feature, the major valley displayed on 22–24 September at Canyonlands and Capitol Reef, also occurs at Bryce and Grand Canyon. Low values for these stations are missing from the plots because poor visual air quality entirely obscured the targets. The poor visual air quality may have been due to low clouds, air pollution, or some combination of both. The other telephotometer targets for these sites did indicate low visibility. Other features which occur simultaneously at many stations include the valley on 2 and 3 October at Canyonlands, Capitol Reef, Chaco Canyon, Bandelier, and White Sands and the peak on 28–30 September at all the stations shown.

The simultaneous visibility events suggest that, at times, the entire visibility network from Canyonlands, Utah to Carlsbad, New Mexico is acting in unison. At other times, perhaps because of local source impacts, visibility events are more localized. However, Grand Canyon appears to be generally representative of the southern Utah/northern Arizona area.

Analysis of the Grand Canyon data was carried out by contrasting characteristics of the days with highest and lowest visual air quality. To do this, a daily geometric mean visual range was computed for two targets at the Grand–Mt. Trumbull, a distant target, and Shiva Saddle, a near target, so that when Mt. Trumbell disappeared because of poor visual air quality, Shiva Saddle could usually be used. These values were sorted and data for days with the 10 highest and 10 lowest visual ranges were identified. Since cloud cover can influence telephotometer data in such a way as to yield anomolously high (bright cumulus cloud behind target) or low (cloud blocking the view of the target) visual ranges (Malm *et al.*, 1979), data for these days were checked using sky conditions determined at the time the measurement was taken and using other locations and targets. When the values appeared to be anomalous, additional trial days were selected from the sorted list and checked, until a total of 10 each "best" and "worst" visibility days were determined (see Table 3).

It is interesting to note that nearly all of the high visibility days are in the fall season while the low visual air quality days are more evenly dispersed throughout the year. However, winter data (not considered here)

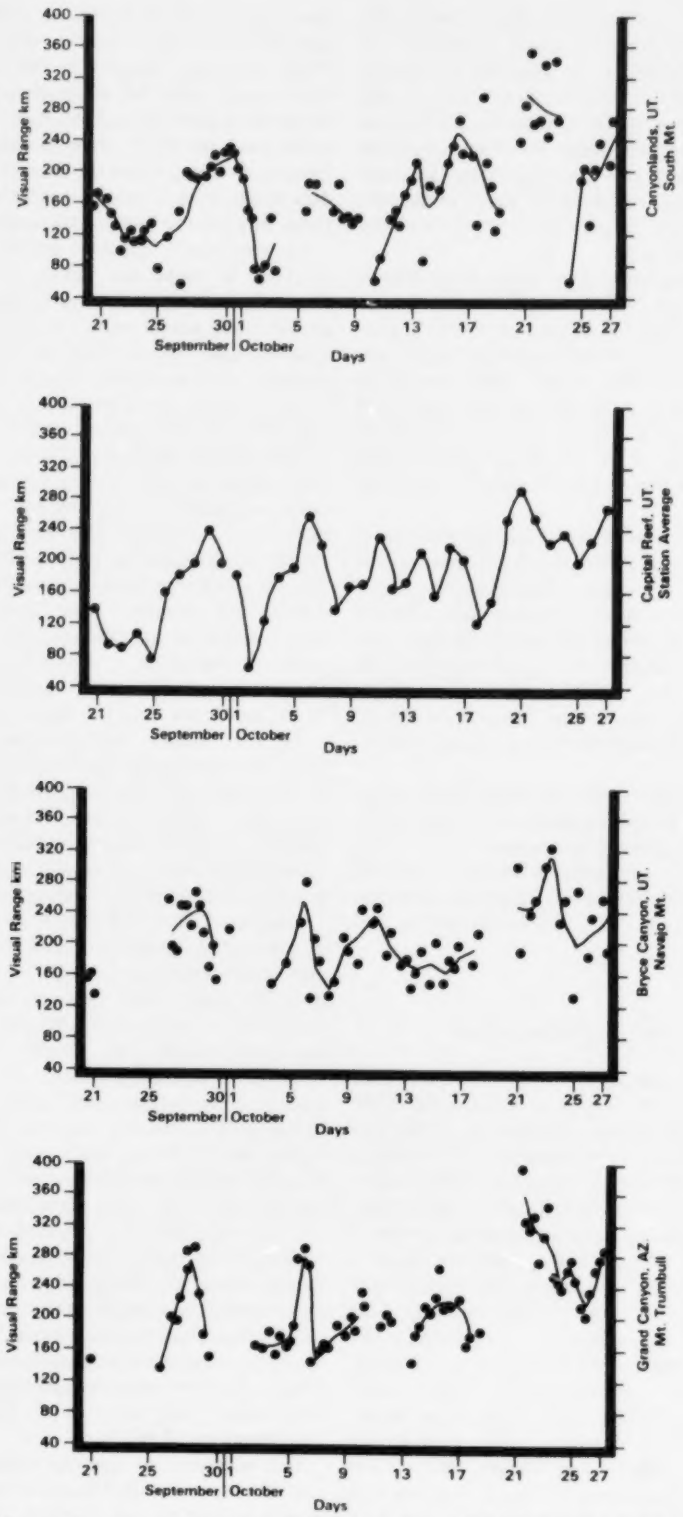

Fig. 2. Visual range time plot for Canyonlands, Capitol Reef, Bryce Canyon and Grand Canyon (21 September–27 October, 1979).

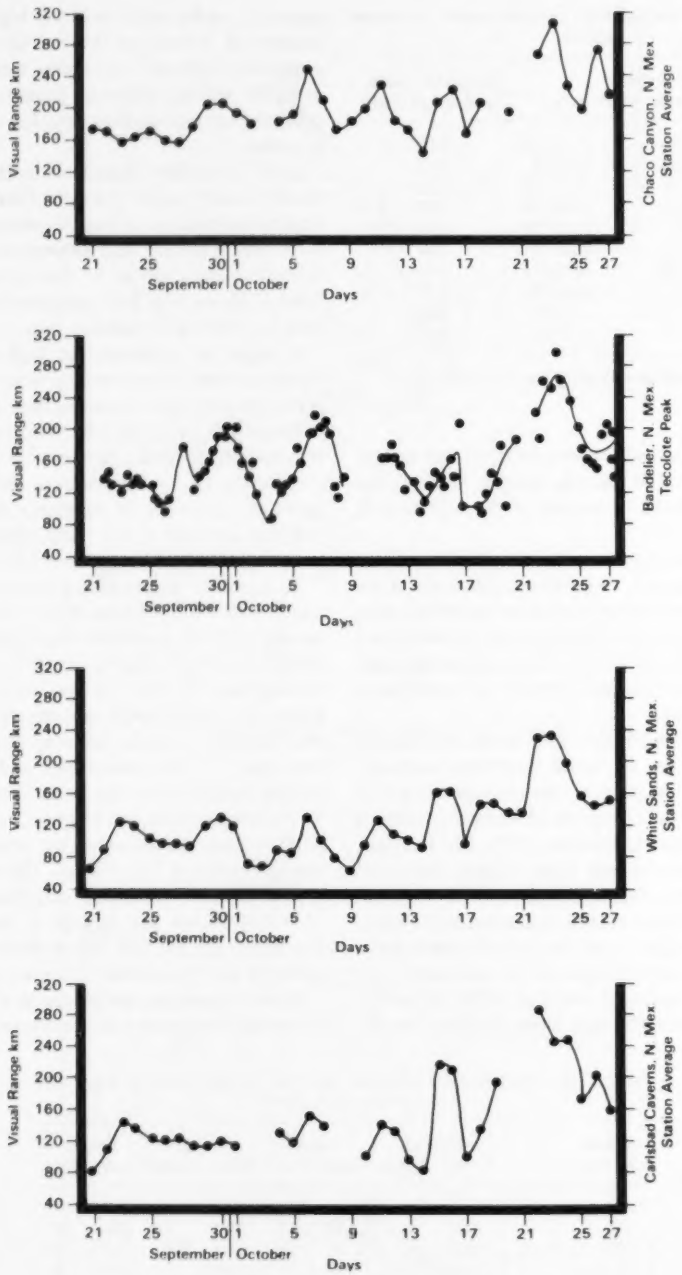

Fig. 3. Visual range time plot for Chaco Canyon, Bandelier, White Sands, and Carlsbad Caverns (21 September–27 October, 1979).

may include some equally high visibility days. Four of the 20 selected dates are contained within the time plots of visual range displayed above. These are 23 October, 22 October, 23 September and 2 October, with mean visual ranges of 335, 332, 69 and 64 km respectively. Generally speaking, these cases of high and low visibility are common to the other locations shown in Figs 2 and 3.

Table 4 lists particle data for the worst and best case visibility days at Grand Canyon for Fall, 1979. Concentrations of copper, lead, sulfur and silicon for the fine stage are given along with the relative ranking

Table 3. Dates of low and high visual air quality at Grand Canyon

Date	Geometric mean visual range (km)*	Date	Geometric mean visual range (km)*
5/18/79	56	11/25/79	310
5/29/79	58	11/1/79	312
7/21/79	60	10/27/78	314
10/2/79	64	10/28/78	315
8/13/79	67	11/29/79	318
9/23/79	69	8/29/79	330
9/11/79	70	10/22/79	332
9/9/79	73	10/23/79	335
9/1/78	73	11/8/78	338
9/10/79	77	11/7/78	349

* Using Shiva Saddle and Mt. Trumbull targets.

(from highest to lowest concentration) of that sample among the total of 61 particle samples taken at the Grand Canyon from 17 August, 1979 to 28 March, 1980.

Sulfur values for the worst case days are among the highest 10% measured, while silicon values are in the highest 20%. Sulfur and silicon values for the best days are about one fifth the concentrations of the worst day values. This is consistent with the relationships suggested by the principal component and correlation coefficient analyses.

Another interesting feature is the variation in copper concentrations. They are below detectable limits except during two time periods, one corresponding to a low visibility case on 2 October, 1979, and the other, a high case on 22 and 23 October, 1979. These copper values are the second and third highest measured. However, it is curious that days with unusually high and low visual air quality should be associated with copper values of nearly equal value. One would expect that a high copper concentration would be associated with copper smelter emissions (Small *et al.*, 1979), and would in turn be associated with high levels of sulfur. Yet, the copper to sulfur ratio is much higher for the high visibility case than for the low case. This could be caused by different conversion rates for sulfur dioxide to sulfate, different primary emission composition, or non-smelter sources of either copper or sulfur.

Lead is another element of interest in that it is usually linked to auto emissions. One might anticipate high concentrations of lead associated with transport from urban centers, and subsequent low visibilities. However, examination of lead concentrations (see Table 4) shows high lead concentrations occurring on both high and low visibility days.

It might be expected that high sulfur, lead and copper concentrations would be associated with transport from geographic areas containing sources of these pollutants. It might also be of interest to determine whether or not there are "clean corridors," i.e., areas over which an air mass moves without picking up significant amounts of pollutants that could reduce visibility. In order to test these questions trajectories were computed for each of the best and worst days.

To calculate trajectories, a version of the Air Research Laboratory Atmospheric Transport and Dispersion (ATAD) model was used (Heffter, 1980). This version calculates trajectories of 3 days in duration, moving back in time, starting every 6 h during any given day. Trajectories are calculated using winds determined for a model-calculated transport layer. The data base for the trajectories and transport layer heights calculated for this paper consists of upper air winds, temperatures, and heights from rawinsonde and pibal stations located within the latitudes of 45–30° N and longitudes of 125–100° W. The model produces a plot of trajectory positions every three hours, for each of 4 trajectories per day on a standard mercator coordinate system. The four trajectories were visually averaged and transferred to a state outline map.

These trajectories are shown in Figs 4 and 5. The extent of the trajectory in hours is shown at the end of

Table 4. Fine particle data for worst and best visibility days at the Grand Canyon (Fall, 1979)

Vis. date/ Part. date*	Copper Conc.†	Copper Rank‡	Lead Conc.	Lead Rank	Sulfur Conc.	Sulfur Rank	Silicon Conc.	Silicon Rank
Worst								
9–9/9–7	BDL	–	55	16	2004	2	606	11
9–10 9–11/9–10	BDL	–	58	14	1957	4	722	9
9–23/9–21	BDL	–	97	5	2058	1	744	8
10–2/10–1	14	2	BDL	–	1756	6	999	6
Best								
10–21/no sample available	–	–	–	–	–	–	–	–
10–22, 23/10–22	12	3	BDL	–	542	18	148	31
11–5/11–5	BDL	–	65	9	412	24	132	32
11–29/11–26	BDL	–	32	21	207	42	379	13

BDL = Below detectable limits.
* = Date of visibility case/first day of 72 h particle sample.
† = Concentration in ng m^{-3}.
‡ = Rank of data from highest to lowest concentration for 61 total cases.

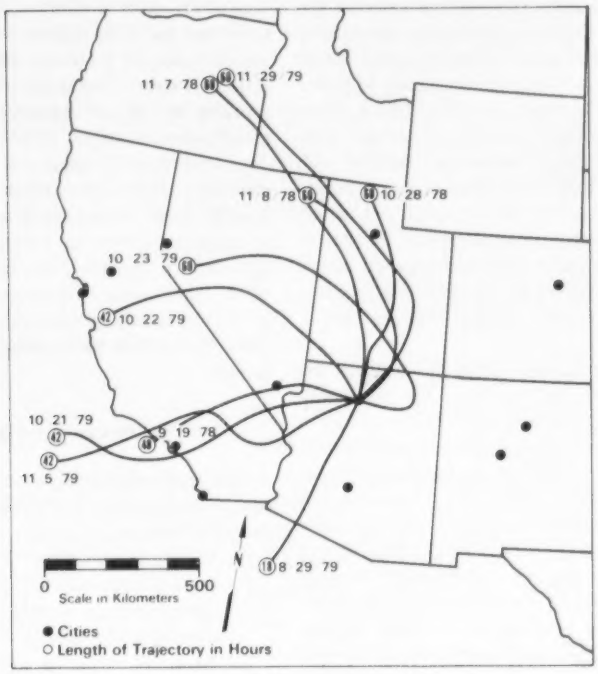

Fig. 4. Wind trajectories back in time for days of high visual air quality.

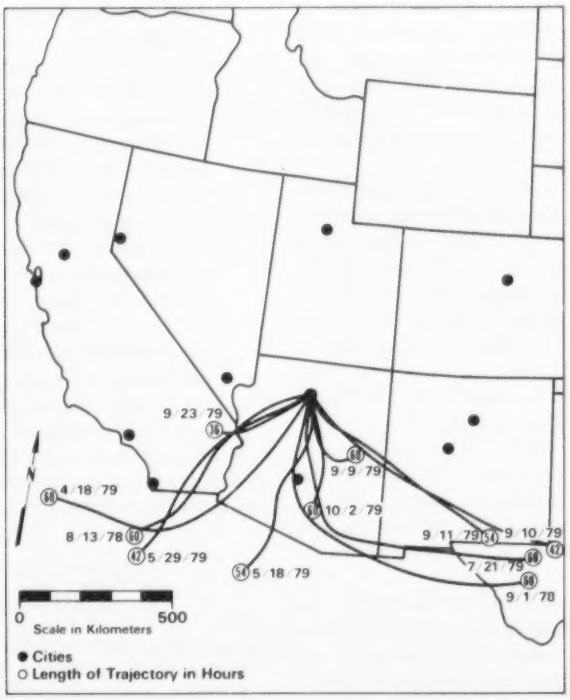

Fig. 5. Wind trajectories back in time for days of low visual air quality.

the trajectory path. Trajectories were truncated at 60 h for display purposes, while trajectories shown with shorter times were truncated by the trajectory model for lack of data. The dates shown correspond to the air parcel arrival time at Grand Canyon. Figure 4 shows days with visual ranges equal to or greater than 310 km, while Fig. 5 shows trajectories for days with visual ranges of less than 80 km. The majority of days of high visual air quality have trajectories which approach Grand Canyon from the north and northwest over largely remote and unpopulated areas. Several trace paths over the Los Angeles metropolitan area, while one traverses western Arizona and a portion of Mexico.

More significantly however, the paths of the worst case air masses never initiate from the northwest. Instead, these trajectories approach the Grand Canyon from the southwest, west, and southeast, passing over central and southern Arizona, southern California, and southern New Mexico. Several may be associated with copper smelter emissions. In fact, the trajectory for 2 October, 1979, when the sixth highest sulfur and the second highest copper concentrations were recorded, passes directly over the central Arizona smelter area. On the other hand, the third highest copper concentration occurs for the particulate sample corresponding to two best case visibility days, 22 and 23 October. Surprisingly enough, the 23 October trajectory passes the McGill, Nevada copper smelter. A check of travel time from the smelter to Grand Canyon for both cases shows it to be approx. 60 h for the first case and 36–48 h for the second. This suggests an additional reason the sulfur values may be low for 22 and 23 October. The sulfur dioxide-to-sulfate conversion time involved may be responsible. This again points out that fine copper may be a suitable tracer for smelter influence though the degree of impact seems to depend on other factors.

Further examination of the trajectory plots shows there are three best day and possibly one worst day trajectories that arrive at Grand Canyon from somewhat similar paths over southern California. Unfortunately, particulate data are not available for two of these days, leaving only a low visibility day, 23 September, 1979, and a high visibility day, 5 November, 1979, which show the fifth and ninth highest lead concentrations respectively. The highest fine sulfur value recorded also occurs for the 22 September sampling period, while in contrast, the sulfur value is low on 5 November. One reason for this difference may be the rain in the Los Angeles area on 3 and 4 November which may have reduced the pollutant concentrations there. No rain occurred for the low visibility case.

Another reason for this difference may be the wind velocities (trajectory length/trajectory duration) and thus, the dilutions experienced by the parcels of air. The high visibility trajectory had a velocity of nearly 3 times greater than the low visibility trajectory, and as a result, spent approx. 2/3 less time over the source area. One of the other southern California best day trajectories has the third highest overall velocity of the 20 cases considered. However, this relationship of overall trajectory velocity to its classification as a high or low visibility day is not generally true. When the mean group velocities of the 10 best and 10 worst visibility days are compared using a t-test, there is no significant difference between the groups at the 90% confidence level. However, it seems reasonable that dilution would be important only when the trajectory has passed over an area with significant sources. Further investigation of the relationship of meteorological conditions such as relative humidity, wind velocity, precipitation, and solar insolation to the trajectories may offer additional insight.

SUMMARY AND CONCLUSIONS

This preliminary analysis of visibility, particle, and meteorological data for project VIEW has shown a variety of interesting results.

(1) Principal component analysis, for Fall 1979 showed that visibility parameters consistently appeared in the same factor with fine sulfur, and usually appeared with coarse soil and particles.
(2) At times, visibility values measured for the entire VIEW network from Canyonlands, Utah to Carlsbad, New Mexico, behave in unison, while at other times, each site behaves independently.
(3) Nearly all of the best visibility days selected for the Grand Canyon occur in the Fall, rather than in Spring and Summer, the other seasons considered. Low visibility days tend to be spread more evenly over these seasons.
(4) Fine copper may be suitable for use as a tracer for determining the influence of copper smelters on visibility at the Grand Canyon. Occurrences of high and low visibility are associated with high copper values.
(5) The existence of a "clean corridor" across parts of central and western Utah, central and northern Nevada, Idaho, and Oregon is suggested by the trajectory analyses. This implies that developments planned for this corridor may have significant impact on visual air quality at the Grand Canyon and other nearby national parks and monuments.

Further research using these and other data is expected to provide a more complete picture of factors controlling visibility in the West.

REFERENCES

Barone J. B., Cahill T. A., Eldred R. A., Flocchini R. G., Shadoan D. J. and Deitz T. M. (1978). A Multivariate Statistical Analysis of Visibility Degradation at Four California Cities. *Atmos. Envir.* **12**, 2213–2221.
Frane J. W. and Hill M. (1974) Annotated Computer Output

for Factor Analysis using Professor Jarvik's Smoking Questionnaire. Technical Report No. 8, Health Sciences Computing Facility, UCLA.

Frane J. W. and Hill M. (1976) Factor analysis as a tool for data analysis. *Commun. Statist.–theor. Meth.*, **A5**, 487–506.

Flocchini R. G., Cahill T. A., Pitchford M. L., Eldred R. A., Feeney P. J. and Ashbaugh L. L. (1981) Characterization of Particles in the Arid West. Presented at Symposium on Plumes and Visibility: Measurements and Model Components, Grand Canyon, November 10–14. *Atmos. Envir.* **15**, 2017–2030.

Garenstroom P. D., Perone S. P. and Moyers J. L. (1977) Application of pattern recognition and factor analysis for the characterization of atmospheric particulate composition in southwest desert atmosphere. *Envir. Sci. Technol.*, **11**, 795.

Heffter J. L. (1980) Atmospheric Transport and Dispersion Model (ARL-ATAD) NOAA Technical Memorandum ERL-ARL-81. Air Resources Lab, Silver Spring Maryland.

Henry R. C. and Hidy G. M. (1979) Multivariate analysis of particulate sulfate and other air quality variables by principal components—Part I. Annual data from Los Angeles and New York. *Atmos. Envir.* **13**, 1581–1596.

Hopke P. K., Gladney E. S., Gordon G. E. and Zoller W. H. (1976) The use of multivariate analysis to identify sources of selected elements in the Boston urban aerosol. *Atmos. Envir.* **10**, 1015–1025.

Jaggard D. L., Hill C., Shorthill R. W., Stuart D., Glantz M., Rosswog F., Taggart B. and Hammond S. (1980) Light Scattering from Sulfates and Soil Dust, presented at Symposium on Plumes and Visibility: Measurements and Models Components, Grand Canyon, November 10–14.

Lyons C. E., Tombach I., Eldred R. A., Terraglio F. P. and Core J. E. (1979) Relating Particulate Matter Sources and Impacts in the Willammette Valley During Field and Slash Burning. Presented at the 72nd Annual Meeting and Exhibition, Cincinnati, Ohio, June 24–29.

Malm W. C. (1979) Considerations in the measurement of visibility *J. Air. Pollut. Control Ass.* **29**(10), 1042–1052.

Malm W. C., Pitchford M. and Archer S. F. (1979) Comparison of electro-optical measurements made by visibility monitoring instruments In: *View on Visibility—Regulatory and Scientific*, edited by Air Pollution Control Association. pp. 222–242.

Malm W. C., Walther E. G., O'Dell K. and Kleine M. (1981) Visibility in the Southwestern United States from Summer 1978 to Spring 1979. Presented at Symposium on Plumes and Visibility: Measurements and Models Components, Grand Canyon, November 10–14. *Atmos. Envir.* **15**, 2031–2042.

Paciga J. J., Roberts T. M. and Jervis R. E. (1975) Particle size distributions of lead, bromine and chlorine in urban–industrial aerosols. *Envir. Sci. Technol.*, **9**, (1), 13.

Pitchford M., Flocchini R. G., Draftz R. G., Cahill T. A., Ashbaugh L. L. and Eldred R. A. Silicon in submicron particles in the southwest. *Atmos. Envir.* **15**, 321–333.

Small M., Germani M. S., Small A. M., Zoller W. H. and Moyers J. L. (1979) An airborne plume study of emissions from the processing of copper ores in Arizona. *Envir. Sci. Technol.* **15**, 293.

Trijonis J. and Yuan K. (1978) Visibility in the Southwest. An Exploration of the Historical Data Base EPA-600/3-78-039.

U.S. EPA (1980) Interim Guidance for Visibility Monitoring Environmental Monitoring and Systems Laboratory, Las Vegas, NV, U.S.A.

APPENDIX

Table A1. Visibility monitoring sites, target numbers used in Fig. 1

Location	Target name	Target No.	Distance (km)
Canyonlands-Island in the Sky	South Mt.	1	50
	Thousand Lake Mt.	4	144
	Mt. Ellen	5	94
Grand Canyon	Shiva Saddle	1	16
	Mt. Trumbull	2	96
	Red Butte	3	28
	Kendrick	4	77
	Desert View Point	5	30
Canyonlands-Hans Flat	Mt. Holmes	1	62
	Mt. Ellen Flank	2	57
	Abajos	5	72
Bryce	Navajo Mt.	1	130
	Table Cliffs Plateau	3	27
	Parker Mt.	4	67
	Cottonwood Peak	5	57
Capitol Reef	Mt. Pennell	2	60
	Ant Hill	3	17
	Repeater Hill	5	20
Dinosaur	Cleveland Peak	1	150
	Rabbit Mt.	3	45
	Book Cliffs	4	76
	Cathedral Bluffs	5	42
Mesa Verde	Lukachuka Mt. 1	1	106
	Chaco River Rise	4	109
	Bridge Timber Mt.	5	47
Wupatki	White Horse Hills	1	34
	Flank of Humphrey	2	33
	Top of Humphrey	3	34

Table A1. cont.

Location	Target name	Target No.	Distance (km)
Navajo	Navajo Mt.	1	48
	Black Mesa 1	3	40
	Black Mesa 2	4	16
Chaco Canyon	Beautiful Mt.	1	105
	Washington Pass	2	94
	Mt. Taylor	5	97
	Nacimiento Mt.	6 (1)	99
Bandelier	Caballo Mt. 2	2	21
	Tecolote Peak	3	65
	Sandia Mt.	4	66
	Thompson Peak	5	45
White Sands	95 Degress	1	30
	Flank of Sierra Blanca	2	69
Carlsbad	Hunter Peak E. Rim	1	46

Table A2. Elements and assumed oxide levels used in particulate mass estimates

Element	Oxide assumed
S	SO_4
Mg	MgO
Al	Al_2O_3
Si	SiO_2
K	K_2O
Ca	CaO
Fe	Fe_2O_2
V	V_2O_5
Mn	MnO
Cu	CuO
Cr	CrO
Ni	NiO
Zn	ZnO